Atmos. Chem. Phys. Discuss., 12, 753–785, 2012
www.atmos-chem-phys-discuss.net/12/753/2012/
doi:10.5194/acpd-12-753-2012

Atmospheric Chemistry and Physics Discussions

Wet and dry deposition of atmospheric nitrogen at ten sites in Northern China

Y. P. Pan, Y. S. Wang, G. Q. Tang, and D. Wu

State Key Laboratory of Atmospheric Boundary Layer Physics and Atmospheric Chemistry, Institute of Atmospheric Physics, Chinese Academy of Sciences, Beijing 100029, China

Received: 9 October 2011 – Accepted: 17 December 2011 – Published: 10 January 2012

Correspondence to: Y. S. Wang (wys@dq.cern.ac.cn)

Published by Copernicus Publications on behalf of the European Geosciences Union.

Abstract

Emissions of reactive nitrogen (N) species can affect surrounding ecosystems via atmospheric deposition. However, few long-term and multi-site measurements have focused on both the wet and the dry deposition of individual N species in large areas of Northern China. Thus, the magnitude of atmospheric deposition of various N species in Northern China remains uncertain. In this study, the wet and dry atmospheric deposition of different N species was investigated during a three-year observation campaign at ten selected sites in Northern China. The results indicate that N deposition levels in Northern China were high with a ten-site, three-year average of 60.6 kg N ha^{-1} yr^{-1}. The deposition levels showed spatial and temporal variation in the range of 28.5–100.4 kg N ha^{-1} yr^{-1}. Of the annual total deposition, 40 % was deposited via precipitation, and the remaining 60 % was comprised of dry-deposited forms. Compared with gaseous N species, particulate N species were not the major contributor of dry-deposited N; they contributed approximately 10 % to the total flux. On an annual basis, oxidized species accounted for 21 % of total N deposition, thereby implying that other forms of gaseous N, such as NH_3, comprised a dominant portion of the total flux. The contribution of NO_3^- to N deposition was enhanced in certain urban and industrial areas. As expected, the total N deposition in Northern China was significantly larger than the values reported by national scale monitoring networks in Europe, North America and East Asia because of high rates of wet deposition and gaseous NH_3 dry deposition. The results have three important implications. First, atmospheric N deposition in Northern China falls within the range of critical loads for temperate forests and grasslands, a threshold above which harmful ecological effects to specified parts of temperate ecosystems often occur. Second, the magnitude, patterns and forms of N deposition will help to inform simulated N addition experiments, which are used to evaluate ecological impacts on receiving ecosystems. Third, the field-based evidence in this unique deposition dataset validates emission inventories of reactive N species and will help policy-makers control atmospheric pollution. Taken together, these findings

ACPD
12, 753–785, 2012

show that NH_3 emissions should be abated to mitigate high N deposition and associated potential impacts on ecosystems in Northern China.

1 Introduction

During the 20th century, humans began to significantly affect the global cycle of nitrogen (N) by fixing N_2, both deliberately for fertilizer production and inadvertently during fossil fuel combustion (Vitousek et al., 1997). The global rate of reactive N production increased from approximately 15 Tg N yr^{-1} in 1860 to 187 Tg N yr^{-1} in 2005; more than half of this recent total was deposited onto the ground (Gruber and Galloway, 2008). Compared with biologically fixed N produced on the continents, atmospherically deposited N is becoming a proportionately larger source of N for terrestrial and aquatic ecosystems worldwide (Galloway et al., 1995). In recent decades, high rates of atmospheric N deposition have been widely documented in Europe (Dise and Wright, 1995), North America (Fenn et al., 1998) and East Asia (Endo et al., 2010). Although elevated N deposition can stimulate plant growth in N-limited regions and cause substantial CO_2 uptake in terrestrial ecosystems (Townsend et al., 1996), there are concerns regarding the negative ecosystem health impacts of excess atmospheric N deposition, such as a loss of biodiversity, eutrophication, N saturation, soil acidification and increased susceptibility to secondary stresses (Liu et al., 2010).

Atmospheric N is deposited via precipitation (wet deposition) and as gases and particles (dry deposition) (Clark and Kremer, 2005). Therefore, it is important to quantify both the wet and the dry deposition of N; otherwise, an extrapolation of the total N deposition flux could yield highly uncertain estimates of potential ecological impacts. Wet deposition is readily estimated by analyzing N species in precipitation (Barile and Lapointe, 2005; Park and Lee, 2002; Xie et al., 2008; Larssen et al., 2006). However, the dry deposition of N is often omitted from observation based flux studies because of the difficulties inherent in directly quantifying the ambient concentrations and deposition velocities of highly reactive N gases and speciated particles (Pryor et al., 1999).

ACPD
12, 753–785, 2012

Because dry deposition can substantially contribute to total N deposition, neglecting dry deposition will result in an underestimation of the total deposition of N onto surfaces (Hill et al., 2005). Alternatively, inferential modeling has been used extensively as an operational tool to compensate for the absence of measured dry deposition data at regional scales (Flechard et al., 2010). With estimates of dry deposition and the use of monitoring networks in Europe (EMEP), North America (CASTNET) and East Asia (EANET), the total deposition flux of N at the national scale can be calculated.

According to the long-term trends observed by these networks, N deposition has leveled off or stabilized in the US and Europe since the late 1980s or early 1990s because of the implementation of stricter legislation to reduce emissions. In contrast, the concentrations of atmospheric reactive N in East Asia have continued to increase every year for the past three decades, mainly because of the increased emissions of NO_x from combustion processes, NH_3 from agricultural production and particulate N from human activities (Zheng et al., 2002). This increase is reflected in the recent finding that the total N deposition flux observed by EANET (10.6 kg N ha^{-1} yr^{-1}) is larger than those reported by CASTNET (5.3 kg N ha^{-1} yr^{-1}) and EMEP (8.7 kg N ha^{-1} yr^{-1}) (Endo et al., 2010), and is supported by peak estimates of N deposition over Central South China with maximum values of 63.5 kg N ha^{-1} yr^{-1} and an average value of 12.9 kg N ha^{-1} yr^{-1} (Lü and Tian, 2007). If current policies in China are fully implemented, the national emissions of NO_x and NH_3 are estimated to increase by 30 % and 57 %, respectively, from 2005 to 2020 (Zhao Y. et al., 2009). Furthermore, increasing emissions of reactive N species are expected to cause increased levels of atmospheric N deposition across most of China, and N deposition is expected to increase by more than 40 % in certain provinces of Central South and Eastern China (Zhao Y. et al., 2009). As one of the most rapidly developing regions in East Asia, Northern China is particularly susceptible to air pollution from increased emissions of reactive N species.

Despite these predicted increase in N deposition, the magnitude and potential impacts of atmospheric N deposition in Northern China remain uncertain because of a paucity of measurements and quantitative knowledge (Lü and Tian, 2007; He et al.,

ACPD
12, 753–785, 2012

2007). Previous studies of N deposition in Northern China have considered the wet deposition and the dry deposition of N species separately (Shen et al., 2009; Zhang et al., 2008). Furthermore, the large-scale spatial variability was not considered in previous studies, which assessed several locations in agricultural areas (Liu et al., 2006). Although N species in gaseous, particulate and rain phases have been measured in various locations in Northern China, relatively few studies have primarily focused on N deposition measurement; rather, such measurements were usually obtained to provide supporting data for another purpose (Meng et al., 2011; Zhang et al., 2007; Tang et al., 2005). Additionally, past work has mainly included short-term studies and has been limited to urban areas. In the absence of long-term and multi-site measurements, the effects of increasing emissions on N deposition in vast regions of China cannot be determined. An assessment that extends beyond a period of three years would contribute to a better understanding of regional atmospheric N deposition and help to identify effective strategies for mitigating N deposition in the future.

The objective of this study was to investigate spatio-temporal variations in the total atmospheric N deposition flux and thereby establish baseline information for future studies in various areas of Northern China. The atmospheric deposition of N species via particles, precipitation and gaseous processes was examined over a three-year sampling period at ten selected sites with varying urban geographies, energy structures and ecosystem types.

2 Materials and methods

2.1 Site descriptions

The study was conducted between December 2007 and November 2010 across Northern China, which is an area of growing concern regarding the effects of increased N emissions on receiving terrestrial and aquatic ecosystems. The ten sites were selected to provide regional information on N deposition and thereby advance our current

ACPD
12, 753–785, 2012

understanding of the effects on different environments. The sites included the two mega cities of Beijing (BJ) and Tianjin (TJ), the two suburban areas of Cangzhou (CZ) and Yangfang (YF), the three industrial sites of Baoding (BD), Tanggu (TG) and Tangshan (TS), the two agricultural areas of Luancheng (LC) and Yucheng (YC) and a rural site at Xinglong (XL). The general location of each site is shown in Fig. 1. The longitudes ranged from 114.69 to 118.20° E, and the latitudes ranged from 36.85 to 40.38° N. The mean annual precipitation ranged from 400 to 800 mm, and the mean annual air temperature was 8–14 °C; Additional detailed descriptions of the ten selected sites can be found elsewhere (Pan et al., 2010a).

2.2 Wet deposition measurements

Daily rainwater and monthly particulate dry deposition samples were collected using a custom wet-dry automatic collector (APS-2B, Changsha Xianglan Scientific Instruments Co., Ltd.). The wet-dry samplers were equipped with a 707 cm^2 aperture and a 177 cm^2 glass bucket to sample wet and particulate dry deposition, respectively. The precipitation sensor opens the collection funnel of the cover device when rainfall begins, and rainwater flows from the funnel into a 15 l plastic bottle. The funnel lid closes automatically when the precipitation ceases and the rainwater has evaporated from the sensor surface. This feature of the collector is highly useful for simultaneously collecting samples of rainwater and deposited particles with minor mixing the two. After sampling, the collection system is systematically cleaned with distilled water. Snow samples were collected using a clean plastic bucket with an inner diameter of 22 cm as soon as possible after the snowfall events. The rainwater and snow samples were filtered, stored and transported according to a previously described procedure (Pan et al., 2010a).

The species and amounts of inorganic N (IN), including NH_4^+, NO_3^- and NO_2^-, in the precipitation samples were determined using an ion chromatography system (Model ICS-90, Dionex Corporation, Sunnyvale, CA, USA) and the standard laboratory procedure of the State Key Laboratory of Atmospheric Boundary Layer Physics and

ACPD
12, 753–785, 2012

Atmospheric Chemistry (Wang et al., 2012). The detection limit (DL) of N for this instrument was 5 $\mu g\,l^{-1}$. The average concentrations of the N species in the field blanks were well below the DL, thereby indicating that no significant contamination of the rain samples occurred during the sampling, handling, filtration or measurement steps. The wet deposition flux of IN ($_w$IN) were obtained by multiplying the volume-weighted concentrations of IN in the precipitation and the amount of precipitation measured by a standard rain gauge at each site.

2.3 Particulate dry deposition measurements

Although the amount of wet deposition can be determined directly from precipitation samples, dry deposition measurements are much more challenging (Wesely and Hicks, 2000). In this study, a polyurethane foam (PUF) filter, used as a surrogate surface, was placed in the glass bucket to collect the dry-deposited airborne particles for chemical analysis (Pan et al., 2010b). During a rain event, the glass bucket for collecting the dry deposition was covered with a lid. After the precipitation ceased, the lid was lifted and rotated to cover the aperture that collected the rainwater; this simultaneously opened the glass bucket to collect dry-deposited particles.

After collection, the chemical composition of the materials in the PUF filters was determined using methods similar to those described previously (Pan et al., 2010b). The PUF filters were conditioned in a dry box at 40 % relative humidity and 25 °C for 24 h to measure the pre- and post-sampling weights and to determine the mass collected on the filters. The dry deposition flux of particulate matter was calculated by dividing the mass by the surrogate surface area during the sampling period. To determine the content of extractable IN in the deposited particles, the PUF filters were cut into ten to twenty equal portions. The water-soluble species were then extracted from three duplicate portions by adding 50 ml of ultrapure water, ultrasonicating for 30–60 min and filtering through a 0.45 µm membrane. Ion chromatography was either performed immediately or the sample was stored in a refrigerator at 4 °C until the analysis. The results from the triplicate samples were averaged after subtraction of the blank and

ACPD
12, 753–785, 2012

were used to estimate the particulate dry deposition flux of IN ($_p$IN). The field blanks did not significantly influence the observed data.

2.4 Gaseous dry deposition measurements

The inferential technique, which combines the measured concentration and a modeled dry deposition velocities (Schwede et al., 2011), was used to estimate the gaseous dry deposition flux of IN ($_g$IN), including NO_2, NO and NH_3. The ambient NO_2, NO_x and NH_3 concentrations were estimated according to the NO_2^- and NH_4^+ levels measured in the extracts of diffusive samplers (Analysts, Italy) by considering the local temperature and humidity conditions of the site, in accordance with the Analysts practical guide (Perrino and Catrambone, 2004; Costabile et al., 2006). Because the NO_2 and NO_x samplers were exposed simultaneously, NO could be calculated as the difference between the two values. Previous comparisons between passive samplers and in situ continuous active analyzers for these reactive N species indicated that the Analysts passive sampler is reliable for such a study (Wu et al., 2010).

The gaseous dry deposition velocity of NO, NO_2 and NH_3 were simulated using the Models-3/Community Multiscale Air Quality (CMAQ) system (Byun and Ching, 1999). This model has proven to be suitable for regional and urban atmospheric pollution and deposition simulations in China (Zhao Y. et al., 2009). The driving meteorological inputs were provided by the fifth-generation NCAR/Penn State Mesoscale Model (MM5).

2.5 Statistics

One-way analysis of variance (ANOVA) and nonparametric tests were conducted to examine the significance of differences in the annual wet and dry deposition flux of N species for all ten sites over the three years of the study. A linear regression analysis was used to investigate relationships between precipitation and the wet deposition of IN. All statistical analyses were performed using the software Origin 8.0 (Origin Lab Corporation, Northampton, MA, USA) and SPSS 11.5 (SPSS Inc., Chicago, IL, USA).

ACPD
12, 753–785, 2012

3 Results

3.1 Wet deposition flux of N species

The mean annual $_{w}$IN at the ten sites during the period from 2008 to 2010 ranged from 16.3 to 28.2 kg N ha^{-1} yr^{-1}, with 63 % to 78 % in the reduced NH_4^+ form (Fig. 2a). The contribution of NO_3^- to the $_{w}$IN (21–36 %) was less than that of NH_4^+, whereas NO_2^- played a minor or insignificant role. The wet deposition flux of NH_4^+ ($_{w}NH_4^+$) was, on average, 2.7-times greater than that of NO_3^- ($_{w}NO_3^-$). This difference was more pronounced in the agricultural sites (LC and YC); thereby indicating that $_{w}NH_4^+$ had a greater contribution to $_{w}$IN in agricultural areas than in urban and industrial areas. The estimated $_{w}$IN varied among the sites; the highest values occurred at the TG site (28.2 kg N ha^{-1} yr^{-1}) followed by the BJ and YC sites (27.9 and 24.8 kg N ha^{-1} yr^{-1}). The $_{w}$IN results were similar for the BD, CZ, LC, TS, YF and TJ sites with values of 23.1, 22.6, 22.2, 21.6, 20.7 and 18.1 kg N ha^{-1} yr^{-1}, respectively. The lowest flux was observed at the rural site, XL (16.3 kg N ha^{-1} yr^{-1}) and as expected, the three-year mean values were also lower at this site (10–42 %). However, the differences were not significant ($p > 0.05$) between the sites or the different years, thus indicating the absence of a geographic trend in the spatial distribution of wet deposition.

The mean monthly wet deposition flux of N species monitored for the three years ranged from 0 to 12.4 kg N ha^{-1} for NH_4^+ and from 0 to 3.9 kg N ha^{-1} for NO_3^- (Fig. 3a,b). The seasonal variations of these two N species were similar at each site: they were higher during the summer than in the spring, autumn or winter, which corresponded with the seasonal distribution of precipitation levels in Northern China. For example, the total $_{w}NH_4^+$ and $_{w}NO_3^-$ throughout the summer (June to August) were, on average, 10.7 and 3.5 kg N ha^{-1}, respectively, for the ten sites during the three-year period; $_{w}NH_4^+$ and $_{w}NO_3^-$, respectively accounted for 66 % and 57 % of the annual $_{w}$IN. The study area received 364 mm of rain during the summer (66 % of the total annual precipitation). The minimum $_{w}$IN level that occurred in the winter season was attributable

ACPD
12, 753–785, 2012

to a decrease in precipitation. In general, a positive relationship between the monthly deposition of N species (NH_4^+ and NO_3^-) and precipitation was observed at each site ($0.57 < r^2 < 0.88$, $p < 0.001$), thereby indicating that the rainfall amount was an important controlling influence on the seasonal trends of wet deposition.

3.2 Dry deposition flux of particulate N species

The largest mean annual $_pIN$ during the period from 2008 to 2010 was observed at the LC site (7.1 kg N ha^{-1} yr^{-1}) followed by the BD, TS, YC and CZ sites, with values of 6.7, 6.6, 6.5 and 6.5 kg N ha^{-1} yr^{-1}, respectively (Fig. 2b). However, differences in the monthly mean values at these sites were not significant ($p > 0.05$). The $_pIN$ was comparable for the BJ, TG, TJ and YF sites with values of 5.6, 5.4, 5.2 and 5.1 kg N ha^{-1} yr^{-1}, respectively; the monthly mean values at these sites were also not significantly different ($p > 0.05$). The lowest annual mean flux was observed at the XL site (4.2 kg N ha^{-1} yr^{-1}), and this result was attributed to the site's rural characteristics. The monthly mean values at this site differed significantly from those at the other sites ($p < 0.05$) with the exception of YF. In general, NH_4^+ (29–72 % of $_pIN$) and NO_3^- (27–70 % of $_pIN$) were the predominant species in the $_pIN$, whereas the contribution of NO_2^- was negligible (less than 11 % of $_pIN$). NH_4^+ was the primary species at most of the sites with the exception of BJ, TJ, TS and YF.

During the three-year period, the monthly mean dry deposition flux of particulate N species ranged from 0 to 1.1 kg N ha^{-1} for NH_4^+ and from 0 to 1.8 kg N ha^{-1} for NO_3^- (Fig. 3c,d). For most sites, the particulate dry deposition flux of NH_4^+ ($_pNH_4^+$) was higher in the winter than in the other seasons, which corresponded to the period of home heating in the target areas. Flux values were lower in August than in the other months, probably as a result of efficient wet deposition. Compared with $_pNH_4^+$, the particulate dry deposition flux of NO_3^- ($_pNO_3^-$) showed a different seasonal variation with a lower flux in the winter than in the other seasons. The $_pNO_3^-$ was notably higher in July, August and September at the BJ site. This pattern was different from that observed at

ACPD
12, 753–785, 2012

the TS site, where the $_pNO_3^-$ peaked in September, October and November, at the TJ, TG, YC and YF sites, where a higher $_pNO_3^-$ was observed during April and June, and at the XL and CZ sites, where the highest $_pNO_3^-$ occurred in October. The $_pNO_3^-$ was elevated in June at the TG site, which was similar to the wet deposition trend.

3.3 Dry deposition flux of gaseous N species

The spatial variations of the mean annual $_gIN$ between 2008 and 2010 are presented in Fig. 2c. The results show relatively high $_gIN$ at the coastal TG site (66.8 kg N ha^{-1} yr^{-1}) and the two agricultural sites, YC and LC (39.3 and 46.3 kg N ha^{-1} yr^{-1}, respectively); relatively low values were observed at the suburban YF site and the rural XL site (16.7 and 8.1 kg N ha^{-1} yr^{-1}, respectively). However, the $_gIN$ was approximately equal at the BD, BJ, CZ, TJ and TS sites with values of 28.5, 25.7, 29.8, 28.9 and 31.7 kg N ha^{-1} yr^{-1}, respectively. In general, the annual mean $_gIN$ values at the TG and LC sites were significantly higher than those at the other eight sites ($p < 0.05$). In contrast, the annual mean $_gIN$ values were significantly lower at the rural XL and suburban YF sites than those at the other eight sites ($p < 0.05$), which is indicative of fewer sources of emissions. The year-to-year variations in the annual average $_gIN$ were comparatively small at each site with the exception of XL, which showed significantly lower values in 2008 than in 2009 or 2010 ($p < 0.05$). The observation of similar $_gIN$ values for different years indicates that emissions were constant from year to year at each site.

Overall, the average gaseous dry deposition of N species in Northern China based on ten sites was 32.2 kg N ha^{-1} yr^{-1} during the period from 2008 to 2010. More than 91 % (84–97 %) of this total was attributed to NH_3. The mean annual molar ratio between NH_3 and NO_2 ranged from 28 to 134, thereby indicating that NH_3 played a more significant role than NO_x in the $_gIN$ for agricultural, rural, suburban and even urban sites. The gaseous dry deposition flux of NH_3 ($_gNH_3$) at the LC and YC sites were 2–3 times higher than those at the urban and industrial sites (BD, TJ, BJ and TS),

ACPD
12, 753–785, 2012

whereas the gaseous dry deposition flux of NO_2 ($_gNO_2$) were similar or lower at these two agricultural sites than at the other sites.

The monthly mean dry deposition flux of gaseous N species during the three-year period ranged from 0.06 to 10.4 kg N ha^{-1} for NH_3 and from 0.02 to 0.57 kg N ha^{-1} for NO_2 (Fig. 3e,f). The seasonal variations of $_gNO_2$ were similar at most sites with higher values measured between May and October. At the XL site, however, the seasonal distribution of $_gNO_2$ was not distinct, thereby indicating that the emissions of NO_2 were constant throughout the entire year. As presented in Fig. 3e, the seasonal trends of $_gNH_3$ at most sites, with the exception of TG, did not significantly differ. All sites showed notable peaks in the summer months (July or August) and lower values in the spring, autumn and winter.

In contrast to the other sites, the $_gNH_3$ values for the TG site in the winter, spring and autumn were significantly elevated relative to the summer values. This finding is different from the other locations, including the urban TJ site. Although the model-estimated gaseous dry deposition velocities from the TJ and TG sites were comparable, the flux estimates were significantly different because of differences in the concentration measurements. This result is supported by the mean NH_3 concentrations at the TG site that were 3.3-, 2.4-, 1.6- and 2.9-times higher than those at the TJ site during the winter, spring, summer and autumn, respectively. These high $_gNH_3$ values at the TG site throughout the year are indicative of complex local emissions from industry, agriculture and other human activities. The difference in NH_3 concentrations between the TG and TJ sites was smaller in the summer than in other seasons because NH_3 at the TG site can be readily converted to NH_4^+ in the summer as a result of the higher relative humidity of the coastal area and wet deposition near the source (Fig. 2a).

ACPD
12, 753–785, 2012

4 Discussion

4.1 Total atmospheric N deposition in Northern China

The current measurements obtained in this study allowed us to systematically evaluate the total (wet plus dry) deposition of IN in Northern China. Previous studies only focused on either the wet or the dry deposition of individual N species (Shen et al., 2009; Zhang et al., 2008). The mean annual total flux of N deposition ranged from 28.5 to 100.4 kg N ha^{-1} yr^{-1} over the three-year sampling period at the ten sites (Table 1). The year-to-year variations in the annual average total flux were not significant at any site ($p < 0.05$), thereby indicating that the emissions of reactive N were constant on an annual basis for each site. The spatial variation of total IN deposition flux was similar to that of gaseous deposition; the values at the BJ, TJ, BD, TS and CZ sites were higher than those at the XL and YF sites and lower than those at the YC, LC and TG sites. The seasonal variations of total IN deposition flux were also similar to those of the gaseous deposition; higher values were observed in the summer (not shown).

The overall mean total IN deposition flux in Northern China was 60.6 kg N ha^{-1} yr^{-1} during the three-year period. This value was significantly higher than previous estimates of the total N deposition in the target area, which ranged from 13 to 20 kg N ha^{-1} yr^{-1} (Lü and Tian, 2007). This discrepancy was attributed to their omission of certain species, such as NH_3, from the synthesis of the observational data. However, when using the integrated total N input (ITNI) system, the total airborne N input into the agro-ecosystems in the North China Plain was estimated to be 83.3 kg N ha^{-1} yr^{-1} (He et al., 2007), which is greater than the results found for the agricultural sites of LC and YC (75.2 and 66.3 kg N ha^{-1} yr^{-1}, respectively) in this study. The relatively high values estimated by the ITNI system are not surprising because the N deposition estimates from this system vary with both the plant development phase and species of crops (Russow and Böhme, 2005). In addition, the total deposition flux of IN in this study was likely underestimated because certain components, such as HNO_3, were not measured; however, their inclusion is not expected to significantly increase the

ACPD
12, 753–785, 2012

total deposition because of their limited contribution (Shen et al., 2009). The estimated total IN deposition flux in Northern China was approximately 6-times higher than that observed by CASTNET, EMEP and EANET (Endo et al., 2010). The higher values are possibly a result of increased N emissions. Because nation-wide emissions of reactive N will continue to rise, Northern China was estimated to receive the maximum N deposition values by the CMAQ simulations (Zhao Y. et al., 2009). Therefore, it is important to evaluate the effects of increasing N deposition on different ecosystems in Northern China.

4.2 Contribution of different pathways to total N deposition flux

The dry deposition of gaseous N species was the primary contributor to total N deposition at most sites, and the contribution ranged from 28 % (XL) to 67 % (TG), averaging 50 %. The mean annual $_g$IN ranged from 8.1 to 66.8, with a mean of 32.6 kg N ha^{-1} yr^{-1} during the three-year period. The $_g$IN was higher at the agricultural sites, YC and LC, and the industrial site, TG. Given the influence of local NH_3 emissions from intensive fertilization, it is not surprising that the $_g$IN at the agricultural LC site reached 44.5 kg N ha^{-1} yr^{-1}. However, the significantly higher $_g$IN at the coastal TG site could be attributable to the influence of reactive N emissions from anthropogenic sources (see above). The influence of fertilization could also explain why the agricultural site, YC, had a relatively high $_g$IN value than the other industrial locations, including BD, TJ and TS; regardless the difference was not significant ($p > 0.05$). The average value of $_g$IN at the two agricultural sites LC and YC was 42.8 kg N ha^{-1} yr^{-1}. This value agrees with the sum of the annual $_g NH_3$ and $_g NO_2$ (approximately 40 kg N ha^{-1} yr^{-1}), which was previously estimated for agricultural regions in China, but it is significantly higher than values from other agricultural areas in the world (Shen et al., 2009; Hu et al., 2007). With the exception of the TG, LC, YF and XL sites, no clear differences were found among the other six sites where the average $_g$IN value was 30.5 kg N ha^{-1} yr^{-1}, which is approximately 7-times higher than the values reported by EMEP and EANET (Endo et al., 2010).

ACPD
12, 753–785, 2012

The wet deposition contributed 28–57 % to the total N deposition with a mean of 40 %, which was 10 % lower than $_{g}$IN. The average $_{w}$IN at ten sites in Northern China was 22.6 kg N ha^{-1} yr^{-1} between 2008 and 2010. This is approximately 5-times greater than the values reported by CASTNET, EMEP and EANET (Endo et al., 2010). The estimated $_{w}$IN values are also greater than those reported for most areas of China except for the Yangtze River Basin where the average is 27 kg N ha^{-1} yr^{-1} (Xie et al., 2008; Zhao X. et al., 2009).

Compared with $_{w}$IN and $_{g}$IN, the proportion of $_{p}$IN to the total N flux was relatively small, ranging from 5 % to 15 % and averaging 10 %. The mean annual $_{p}$IN ranged from 4.2 to 7.1 with a mean of 5.9 kg N ha^{-1} yr^{-1} during the three-year period. This result is comparable to values from the North China Plain (1.3–9.6kg N ha^{-1} yr^{-1}) obtained as the difference between the bulk and wet-only deposition (Zhang et al., 2008), from Southeast China (3.4–7.6 kg N ha^{-1} yr^{-1}), which was estimated using a water-surrogate surface (Chen et al., 2006), and from other areas around the world, such as Singapore (5.9 kg N ha^{-1} yr^{-1}) (He et al., 2011) and Japan (~5 kg N ha^{-1} yr^{-1}) (Endo et al., 2010), which were estimated using the inferential method.

Precipitation, particulates and gas dry deposition of N, respectively accounted for 40 %, 10 % and 50 % of the total N deposition in Northern China. To our knowledge, the only other simultaneous determination of these three pathways in China showed that the largest sources of atmospheric N to the forest ecosystem in South China was gas (64 %), followed by rainwater (25 %) and particles (11 %) (Hu et al., 2007). The results from this study suggest that wet deposition cannot be used alone to determine the total deposition because the total deposition may be underestimated if the dry deposition of certain species or pathways is not considered. Because dry deposition in both the particulate and gaseous phases are important contributions to total N deposition, additional research is needed to refine the quantities of dry deposition flux. This present study is a significant step in this direction.

ACPD
12, 753–785, 2012

4.3 Effects of the precipitation amount on the wet deposition of N species

A positive relationship between the monthly wet deposition of N species (NH_4^+ and NO_3^-) and precipitation was found. This relationship is similar to that observed between dissolved organic carbon and the amount of precipitation in the target areas (Pan et al., 2010a). Previous studies have also reported consistent precipitation effects on the wet deposition of N and other soluble species (Zhao X. et al., 2009; Zhang et al., 2008; Guo et al., 2008), thus suggesting that the amount of rainfall influences the seasonal trends of wet deposition at a given site. However, the wet deposition of N species in June through September fluctuated dramatically between the sites, and differences between the precipitation and deposition trends were observed (not shown). These monthly fluctuations could be partially explained by the variable amounts of precipitation. However, differences in the precursor atmospheric concentrations of N species are also contributing factors.

To evaluate the influence of anthropogenic emissions on the wet deposition flux of N species, we assumed that the scavenging ratio and the atmospheric concentrations of N compounds were constant at all sites; therefore, the precipitation amounts determined the wet deposition patterns at a regional scale. However, for the sites with higher concentrations of pollutants, the wet deposition flux was greater than those expected from the amount of precipitation based on the above assumption (Sakata et al., 2006). The statistical analysis of data from the three-year period revealed a positive relationship between the annual $_w$IN, particularly between the $_w NH_4^+$ and the corresponding precipitation amounts ($p < 0.01$) (Fig. 4). However, only 35 % and 44 % of the variance of the $_w$IN ($r^2 = 0.35$) and $_w NH_4^+$ ($r^2 = 0.44$), respectively, was explained by the amount of precipitation. The results suggest marked differences in the scavenging ratio and the atmospheric concentrations of N compounds across Northern China. Specifically, the $_w NH_4^+$ values at the BJ, LC and TS sites in certain years tended to be much higher than those expected from the precipitation amount, thereby indicating a large contribution of anthropogenic emissions. However, the relatively low $_w NH_4^+$ values at the XL site

ACPD
12, 753–785, 2012

compared with those expected from the precipitation amount may be due to the lower number of anthropogenic sources in the rural areas. In contrast to the $_{w}IN$ and $_{w}NH_4^+$ trends, the annual $_{w}NO_3^-$ values were not significantly correlated with the precipitation amount (Fig. 4), likely because the annual $_{w}NO_3^-$ values were strongly dependent on local and regional anthropogenic sources.

4.4 Source information of atmospheric N deposition

To obtain additional source information on the wet deposition at the local scale, the molar ratio of NH_4^+/NO_3^- was calculated and is presented in Fig. 2a. The molar ratio of NH_4^+/NO_3^- varied between 1.8 (YF) and 3.3 (LC), and the average was 2.7. The results indicate that NH_3 from agriculture and human and animal excrement remains the major contributor to wet N deposition in the target areas, compared with the NO_3^- from fossil fuel combustion in industry and transportation (Fahey et al., 1999). This fact was more pronounced at the agricultural sites, YC and LC, than at certain industrial and urban sites such as BD, TJ and TS. However, for the wet N deposition, the contribution from NO_3^- was relatively more important at the BJ, XL and YF sites than that from NH_4^+, considering that the ratio of NH_4^+/NO_3^- at these sites was comparable to or much lower than the values at the other sites. Of note is the $_{w}NO_3^-$ in certain months at the mega city BJ site (April, June–September) and its suburban YF site (May and June) had high values relative to most sites (Fig. 3b). This result further reflects the effects of NO_x emissions from industry and transportation in urban areas. However, when compared with values at the other sites, the $_{w}NH_4^+$ and $_{w}NO_3^-$ values were especially elevated in June at the TG site, which was likely the result of local anthropogenic sources.

The molar NH_4^+/NO_3^- ratio was also calculated to investigate the relative contribution of agriculture versus industry and transportation contributions to the dry deposition of particulate N species (Fig. 2b). Relative to wet deposition, industry and transportation emissions appeared to have a greater impact on the composition of dry deposited particulate N. First, the spatial variations of NH_4^+ and NO_3^- differed, thereby indicating

ACPD
12, 753–785, 2012

different sources. Second, the NH_4^+/NO_3^- ratio at each site was lower than that of wet deposition. Third, NO_3^- played a greater role than NH_4^+ in $_pIN$ at the BJ, TJ, TS and YF sites where the NH_4^+/NO_3^- was less than 1. This result is not surprising because these sites are strongly affected by NO_x emissions from industry and transportation. The chemical composition of dry deposited particulate N was different from that of the wet deposited form at these sites, thus reflecting the intense perturbation of the atmospheric N cycle by anthropogenic activities. However, the ratio was greater than 1 at the BD, LC, CZ, YC, TG and XL sites which indicates that particulate NH_4^+ from agriculture and human and animal excrement was the major contributor to $_pIN$. The NH_4^+/NO_3^- ratio at the YC and LC sites reached 2.6, which is twice that of the remaining four sites and implies that the $_pIN$ value in the agricultural regions was mainly dominated by NH_3 from agricultural activities and not by NO_x from industrial activities. This finding agrees with the wet deposition results for agricultural regions.

Surprisingly, the molar ratio of gaseous NH_3 to NO_2 was high at all sites, thereby indicating that NH_3 played a greater role than NO_x in $_gIN$ in Northern China (Fig. 2c). The relatively high $_gNH_3$ could be a result of agriculture and human and animal excrement in the target areas. This conclusion is further supported by the correlation between the seasonal variation of gaseous NH_3 depositions and emissions, both of which are closely related to the timing of fertilization and seasonal changes of temperature (Zhang et al., 2011; Shen et al., 2011). However, the NH_3 emissions from vehicles in urban areas could also contribute to the observed summer maximum (Ianniello et al., 2010).

4.5 Implications of the unique N deposition dataset

The results presented here have three important implications. First, the results show that N is deposited at high levels and may result in significant atmospheric N inputs to surrounding regions. Although the total atmospheric N deposition values (28.5–100.4 kg N ha^{-1} yr^{-1}) are within the range of empirical critical loads

ACPD
12, 753–785, 2012

(10–150 kg N ha^{-1} yr^{-1}) for certain temperate forests and grasslands in north part of China (Liu et al., 2010), they are much higher than the critical loads calculated from the steady state mass balance in the target areas (15–30 kg N ha^{-1} yr^{-1}) (Duan et al., 2001). This result raises concerns regarding the harmful biological and chemical effects on ecosystems, including physiological variations, reduced biodiversity, elevated nitrate leaching, and changes in soil microorganisms (Liu et al., 2010). Although N deposition is an important nutrient resource in the agricultural areas (He et al., 2007), it may also result in the enhanced emissions of nitrous oxide (N_2O) (Zhang et al., 2011), which is an important greenhouse gas. Moreover, coastal waters near industrial regions, such as Bohai Bay, may receive greater nitrogen loads from atmospheric deposition and are susceptible to eutrophication (Barile and Lapointe, 2005; He et al., 2011); e.g., N deposition at the coastal industrial TG site reached 100.4 kg N ha^{-1} yr^{-1}. Thus, the potential risks of heavy N deposition on sensitive terrestrial and aquatic ecosystems should be controlled to within acceptable levels by substantially reducing the amount of reactive N emitted into the atmosphere.

Additionally, the results reported here will inform simulated N deposition experiments. To study the effects of N deposition on ecosystems, simulated N deposition experiments have been conducted for numerous grassland and forest ecosystems in China (Xia et al., 2009; Mo et al., 2007). However, specific conditions in these studies must be addressed. First, the minimum dose of N added to the fields was equal to or several times higher than the estimated atmospheric N deposition (2–53 kg N ha^{-1} yr^{-1}) (Liu et al., 2010), which was most likely an underestimate. Second, most of the N fertilizer was manually sprayed onto the ground (Mo et al., 2007) in the assumption that atmospheric N species were only deposited as rainfall. Compared with the $_p$IN, however, both $_w$IN and $_g$IN are major contributors to the total N deposition at most sites. Thus, the above assumptions ignore the direct effects of gaseous dry deposition on plants, and they may not be applicable to certain natural ecosystems (Sheppard et al., 2011). Lastly, the N addition experiments were usually conducted with NO_3^--N, NH_4^+-N or both (Xia et al., 2009; Mo et al., 2007). Because the dry and the wet deposition of IN are

ACPD
12, 753–785, 2012

dominated by NH_3 and NH_4^+, the reduced N species (NH_y) was found to contribute 71–88 % of the total N flux, whereas the oxidized species (NO_y) constituted only 12–29 % (Table 1). This finding indicates that N deposition is dependent not only on the pathway but also on chemical form, thereby further highlighting the need to better resolve the relative inputs of oxidized and reduced forms of N in simulated experiments.

Finally, the field-based evidence from this study validates the emission data and has significant implications for policy-makers that are attempting to control atmospheric pollution in Northern China. The mean annual deposition flux of NH_y and NO_y during the three-year period were categorized into five grades and plotted on the maps showing the spatial distribution of emissions for the corresponding gases (Fig. 5a,c). The NH_3 emission data included human and livestock excrement, agricultural applications and sewage treatment plants, whereas the NO_x data included vehicles, power plants and industrial and residential sources for the year 2008 at a resolution of $9 \times 9\,km^2$ (Tang, 2010).

NH_y deposition at the rural XL site was the lowest ($20.6\,kg\,N\,ha^{-1}\,yr^{-1}$) of all the sites, which is consistent with the regional background characteristics of the site (Fig. 5a). The emission data shown in Fig. 5a reveal a little amount of NH_3 emissions over the vast mountainous areas to the north and west of Beijing. The NH_y deposition values at the suburban YF site ($30.0\,kg\,N\,ha^{-1}\,yr^{-1}$) were higher than those at the XL site, which was possibly as a result of urban plumes. In contrast, the highest NH_y deposition rate ($87.0\,kg\,N\,ha^{-1}\,yr^{-1}$) was found at the TG site, which is not surrounded by large NH_3 emission sources in Fig. 5a, thus indicating that the inventory did not adequately account for NH_3 emissions from complex sources, such as industry, agriculture and human activities. The second highest NH_y deposition values were observed at the LC site ($66.1\,kg\,N\,ha^{-1}\,yr^{-1}$), followed by the YC, CZ, TS, BD, BJ and TJ sites, with values of 61.3, 48.3, 46.7, 46.1, 42.7 and $40.9\,kg\,N\,ha^{-1}\,yr^{-1}$, respectively. Overall, the spatial pattern of NH_y deposition reflected changes in NH_3 emission sources (Fig. 5b).

The extent of spatial variability of NO_y deposition shown in Fig. 5c was not as large as that of NH_y (Fig. 5a), possibly because NO_x has fewer natural emission sources

ACPD
12, 753–785, 2012

than NH_3. Similar to NH_y, the lowest NO_y deposition values (7.9 kg N ha^{-1} yr^{-1}) were also observed at the rural XL site as a result of fewer anthropogenic emissions. This difference in sources could also explain why the agricultural sites YC and LC had relatively low NO_y deposition levels compared with the suburban sites CZ and YF. However, NO_y deposition was much higher at the urban and industrial areas, including BJ, BD, TG and TS, where power plant, industry and transportation emissions of NO_x were also larger than in the surrounding regions, as shown in Fig. 5c. NO_y deposition was significantly higher at BJ than at TJ, whereas NO_x emissions were lower at BJ than at TJ (Fig. 5d). Because the BJ site is close to roads, vehicle emissions may be the major source of NO_x, and these emissions may be underestimated in existing inventories.

The spatial patterns of observed NH_y and NO_y deposition were similar to NH_3 and NO_x emissions, respectively. Additionally, NH_3 emissions were greater than those of NO_x in large areas (Fig. 5a, c), which agree with the field-based evidence mentioned above. Although the magnitudes of the emissions were not necessarily proportional to the field measurements of deposition (Fig. 5b, d), the applicability of the emissions data cannot be discounted. If combined with deposition data, emissions inventory can be used to distinguish approximate regional differences in reactive N pollution and help policy-makers implement source control decisions. To mitigate atmospheric N deposition in Northern China and its potential ecological impacts, reactive N emissions, especially NH_3 surrounding the BJ, TS and LC sites, must be abated.

5 Conclusions

Our study is among the first to investigate both the dry and the wet deposition of individual N species in Northern China. This unique dataset provides field-based evidence that the total atmospheric N deposition is significantly higher than previous estimates in the target area and in other regions of the world. Further, the observed values are within the range of critical loads for temperate forests and grasslands, thus prompting concerns regarding ecological impacts. The major results and conclusions are as follows.

ACPD
12, 753–785, 2012

1. Clear seasonal variations were observed, although spatial differences in the wet deposition flux of the N species were not significant in Northern China between the ten sites or in the different years. The precipitation amount, scavenging ratio and the atmospheric concentrations of N compounds significantly influenced the annual $_{w}$IN throughout Northern China.

2. The seasonal and spatial variations of dry deposition flux for gaseous N species were significantly, however, the variations in particulate N species were not significant. The greatest contribution to the total N deposition was from $_{g}$IN, followed by $_{w}$IN and $_{p}$IN.

3. The atmospheric deposition flux of NH_y was greater than that of NO_y. Human activities had greater significant impacts on the deposition of NO_y than NH_y at certain urban and industrial sites, which is in agreement with NH_3 and NO_x emission data.

4. The magnitudes, pathways and species of deposited N have significant implications for simulated N deposition experiments. To mitigate N deposition risks to sensitive terrestrial and aquatic ecosystems in Northern China, priority should be given to strategies for bringing NH_3 emissions to within acceptable levels.

Acknowledgements. This work was supported by the Knowledge Innovation Project of the Chinese Academy of Sciences (No.: KZCX1-YW-06-01), the National Natural Science Foundation of China (No.: 41021004) and the National Basic Research Program of China (No.: 2007CB407303). The authors would like to thank H. Tang, W. Liu, W. Wang, G. Fu, Y. Chang, X. Feng, Y. Cheng, C. Zhang, Z. Liu and other staff at the ten monitoring sites for their cooperation during sample collection. We also thank X. Zheng in the Institute of Atmospheric Physics, CAS for her invaluable comments.

ACPD
12, 753–785, 2012

References

Barile, P. J. and Lapointe, B. E.: Atmospheric nitrogen deposition from a remote source enriches macroalgae in coral reef ecosystems near Green Turtle Cay, Abacos, Bahamas, Mar. Pollut. Bull., 50, 1262–1272, doi:10.1016/j.marpolbul.2005.04.031, 2005.

Byun, D. W. and Ching, J. K. S.: Science algorithms of the EPA Models-3 community multi-scale air quality (CMAQ) modeling system, Report EPA/600/R-99/030, US Environmental Protection Agency, Research Triangle Park, NC, 1999.

Chen, N. W., Hong, H. S., Xiao, J., Zhang, L. P., and Wang, J. P.: Dry deposition of atmospheric nitrogen to Jiulong River watershed in Southeast China, Acta Ecol. Sin., 26, 2602–2067 (in Chinese), 2006.

Clark, H. and Kremer, J. N.: Estimating direct and episodic atmospheric nitrogen deposition to a coastal waterbody, Mar. Environ. Res., 59, 349–366, doi:10.1016/j.marenvres.2004.06.001, 2005.

Costabile, F., Bertoni, G., Desantis, F., Wang, F., Weimin, H., Fenglei, L., and Allegrini, I.: A preliminary assessment of major air pollutants in the city of Suzhou, China, Atmos. Environ., 40, 6380–6395, doi:10.1016/j.atmosenv.2006.05.056, 2006.

Dise, N. B. and Wright, R. F.: Nitrogen leaching from European forests in relation to nitrogen deposition, Forest Ecol. Manag., 71, 153–161, doi:10.1016/0378-1127(94)06092-W, 1995.

Duan, L., Xie, S., Zhou, Z., Ye, X., and Hao, J.: Calculation and mapping of critical loads for S, N and acidity in China, Water Air Soil Poll., 130, 1199–1204, doi:10.1023/A:1013908629150, 2001.

Endo, T., Yagoh, H., Sato, K., Matsuda, K., Hayashi, K., Noguchi, I., and Sawada, K.: Regional characteristics of dry deposition of sulfur and nitrogen compounds at EANET sites in Japan from 2003 to 2008, Atmos. Environ., 45, 1259–1267, doi:10.1016/j.atmosenv.2010.12.003, 2010.

Fahey, T. J., Williams, C. J., Rooney-Varga, J. N., Cleveland, C. C., Postek, K. M., Smith, S. D., and Bouldin, D. R.: Nitrogen deposition in and around an intensive agricultural district in Central New York, J. Environ. Qual., 28, 1585–1600, 1999.

Fenn, M. E., Poth, M. A., Aber, J. D., Baron, J. S., Bormann, B. T., Johnson, D. W., Lemly, A. D., McNulty, S. G., Ryan, D. F., and Stottlemyer, R.: Nitrogen excess in North American ecosystems: predisposing factors, ecosystem responses, and management strategies, Ecol. Appl., 8, 706–733, doi:10.2307/2641261, 1998.

ACPD
12, 753–785, 2012

Flechard, C. R., Nemitz, E., Smith, R. I., Fowler, D., Vermeulen, A. T., Bleeker, A., Erisman, J. W., Simpson, D., Zhang, L., Tang, Y. S., and Sutton, M. A.: Dry deposition of reactive nitrogen to European ecosystems: a comparison of inferential models across the NitroEurope network, Atmos. Chem. Phys., 11, 2703–2728, doi:10.5194/acp-11-2703-2011, 2011.

Galloway, J. N., Schlesinger, W. H., Hiram Levy, I. I., Michaels, A., and Schnoor, J. L.: Nitrogen fixation: anthropogenic enhancement-environmental response, Global Biogeochem. Cy., 9, 235–252, doi:10.1029/95GB00158, 1995.

Gruber, N. and Galloway, J. N.: An Earth-system perspective of the global nitrogen cycle, Nature, 451, 293–296, doi:10.1038/nature06592, 2008.

Guo, Y., Feng, X., Li, Z., He, T., Yan, H., Meng, B., Zhang, J., and Qiu, G.: Distribution and wet deposition fluxes of total and methyl mercury in Wujiang River Basin, Guizhou, China, Atmos. Environ., 42, 7096–7103, doi:10.1016/j.atmosenv.2008.06.006, 2008.

He, C. E., Liu, X. J., Fangmeier, A., and Zhang, F. S.: Quantifying the total airborne nitrogen input into agroecosystems in the North China Plain, Agr. Ecosyst. Environ., 121, 395–400, doi:10.1016/j.agee.2006.12.016, 2007.

He, J., Balasubramanian, R., Burger, D. F., Hicks, K., Kuylenstierna, J. C. I., and Palani, S.: Dry and wet atmospheric deposition of nitrogen and phosphorus in Singapore, Atmos. Environ., 45, 2760–2768, doi:10.1016/j.atmosenv.2011.02.036, 2011.

Hill, K. A., Shepson, P. B., Galbavy, E. S., and Anastasio, C.: Measurement of wet deposition of inorganic and organic nitrogen in a forest environment, J. Geophys. Res., 110, G02010, doi:10.1029/2005jg000030, 2005.

Hu, Z. Y., Xu, C. K., Zhou, L. N., Sun, B. H., He, Y. Q., Zhou, J., and Cao, Z. H.: Contribution of atmospheric nitrogen compounds to N deposition in a broadleaf forest of Southern China, Pedosphere, 17, 360–365, doi:10.1016/S1002-0160(07)60043-5, 2007.

Ianniello, A., Spataro, F., Esposito, G., Allegrini, I., Rantica, E., Ancora, M. P., Hu, M., and Zhu, T.: Occurrence of gas phase ammonia in the area of Beijing (China), Atmos. Chem. Phys., 10, 9487–9503, doi:10.5194/acp-10-9487-2010, 2010.

Larssen, T., Lydersen, E., Tang, D., He, Y., Gao, J., Liu, H., Duan, L., Seip, H., Vogt, R., and Mulder, J.: Acid rain in China, Environ. Sci. Technol., 40, 418–425, doi:10.1021/es0626133, 2006.

Liu, X., Ju, X., Zhang, Y., He, C., Kopsch, J., and Fusuo, Z.: Nitrogen deposition in agroecosystems in the Beijing area, Agr. Ecosyst. Environ., 113, 370–377, doi:10.1016/j.agee.2005.11.002, 2006.

ACPD
12, 753–785, 2012

Liu, X. J., Duan, L., Mo, J. M., Du, E., Shen, J. L., Lu, X. K., Zhang, Y., Zhou, X. B., He, C. E., and Zhang, F. S.: Nitrogen deposition and its ecological impact in China: an overview, Environ. Pollut., 155, 2251–2264, doi:10.1016/j.envpol.2010.08.002, 2010.

Lü, C. Q. and Tian, H. Q.: Spatial and temporal patterns of nitrogen deposition in China: synthesis of observational data, J. Geophys. Res., 112, D22S05, doi:10.1029/2006JD007990, 2007.

Meng, Z. Y., Lin, W. L., Jiang, X. M., Yan, P., Wang, Y., Zhang, Y. M., Jia, X. F., and Yu, X. L.: Characteristics of atmospheric ammonia over Beijing, China, Atmos. Chem. Phys., 11, 6139–6151, doi:10.5194/acp-11-6139-2011, 2011.

Mo, J., Zhang, W., Zhu, W., Fang, Y., Li, D., and Zhao, P.: Response of soil respiration to simulated N deposition in a disturbed and a rehabilitated tropical forest in Southern China, Plant Soil, 296, 125–135, doi:10.1007/s11104-007-9303-8, 2007.

Pan, Y. P., Wang, Y. S., Xin, J. Y., Tang, G. Q., Song, T., Wang, Y. H., Li, X. R., and Wu, F. K.: Study on dissolved organic carbon in precipitation in Northern China, Atmos. Environ., 44, 2350–2357, doi:10.1016/j.atmosenv.2010.03.033, 2010a.

Pan, Y. P., Wang, Y. S., Yang, Y. J., Wu, D., Xin, J. Y., and Fan, W. Y.: Determination of trace metals in atmospheric dry deposition with a heavy matrix of PUF by inductively coupled plasma mass spectroscopy after microwave digestion, Environ. Sci., 31, 553–559 (in Chinese), 2010b.

Park, S. U. and Lee, Y. H.: Spatial distribution of wet deposition of nitrogen in South Korea, Atmos. Environ., 36, 619–628, doi:10.1016/S1352-2310(01)00489-7, 2002.

Perrino, C. and Catrambone, M.: Development of a variable-path-length diffusive sampler for ammonia and evaluation of ammonia pollution in the urban area of Rome, Italy, Atmos. Environ., 38, 6667–6672, doi:10.1016/j.atmosenv.2004.08.032, 2004.

Pryor, S. C., Barthelmie, R. J., and Jensen, B.: Nitrogen dry deposition at an AmeriFlux site in a hardwood forest in the MidWest, Geophys. Res. Lett., 26, 691–694, doi:10.1029/1999GL900066, 1999.

Russow, R. and Böhme, F.: Determination of the total nitrogen deposition by the ^{15}N isotope dilution method and problems in extrapolating results to field scale, Geoderma, 127, 62–70, doi:10.1016/j.geoderma.2004.11.015, 2005.

Sakata, M., Marumoto, K., Narukawa, M., and Asakura, K.: Regional variations in wet and dry deposition fluxes of trace elements in Japan, Atmos. Environ., 40, 521–531, doi:10.1016/j.atmosenv.2005.09.066, 2006.

ACPD
12, 753–785, 2012

Schwede, D., Zhang, L., Vet, R., and Lear, G.: An intercomparison of the deposition models used in the CASTNET and CAPMoN networks, Atmos. Environ., 45, 1337–1346, doi:10.1016/j.atmosenv.2010.11.050, 2011.
Shen, J., Liu, X., Fangmeier, A., Goulding, K., and Zhang, F.: Atmospheric ammonia and particulate ammonium from agricultural sources in the North China Plain, Atmos. Environ., 45, 5033–5041, doi:10.1016/j.atmosenv.2011.02.031, 2011.
Shen, J. L., Tang, A. H., Liu, X. J., Fangmeier, A., Goulding, K. T. W., and Zhang, F. S.: High concentrations and dry deposition of reactive nitrogen species at two sites in the North China Plain, Environ. Pollut., 157, 3106–3113, doi:10.1016/j.envpol.2009.05.016, 2009.
Sheppard, L. J., Leith, I. D., Mizunuma, T., Neil Cape, J., Crossley, A., Leeson, S., Sutton, M. A., van Dijk, N., and Fowler, D.: Dry deposition of ammonia gas drives species change faster than wet deposition of ammonium ions: evidence from a long-term field manipulation, Glob. Change Biol., 17, 3589–3607, doi:10.1111/j.1365-2486.2011.02478.x, 2011.
Tang, A., Zhuang, G., Wang, Y., Yuan, H., and Sun, Y.: The chemistry of precipitation and its relation to aerosol in Beijing, Atmos. Environ., 39, 3397–3406, doi:10.1016/j.atmosenv.2005.02.001, 2005.
Tang, G. Q.: Modelling of ozone spatial-temporal distribution in the vicinity of Beijing during Olympics, Ph.D. thesis, Institute of Atmospheric Physics, Chinese Academy of Sciences, Beijing, 153 pp., 2010.
Townsend, A., Braswell, B., Holland, E., and Penner, J.: Spatial and temporal patterns in terrestrial carbon storage due to deposition of fossil fuel nitrogen, Ecol. Appl., 6, 806–814, doi:10.2307/2269486, 1996.
Vitousek, P., Mooney, H., Lubchenco, J., and Melillo, J.: Human domination of Earth's ecosystems, Science, 277, 494–499, doi:10.1126/science.277.5325.494, 1997.
Wang, Y., Yu, W., Pan, Y., and Wu, D.: Acid neutralization of precipitation in Northern China, J. Air. Waste. Manage., in press, 2012.
Wesely, M. L. and Hicks, B. B.: A review of the current status of knowledge on dry deposition, Atmos. Environ., 34, 2261–2282, doi:10.1016/s1352-2310(99)00467-7, 2000.
Wu, D., Wang, Y. S., Pan, Y. P., Xin, J. Y., and Tang, G. Q.: Application of passive sampler to monitor and study atmospheric trace gases in Beijing-Tianjin-Hebei area, Environ. Sci., 31, 2844–2851 (in Chinese), 2010.
Xia, J., Niu, S., and Wan, S.: Response of ecosystem carbon exchange to warming and nitrogen addition during two hydrologically contrasting growing seasons in a temperate steppe,

ACPD
12, 753–785, 2012

Glob. Change Biol., 15, 1544–1556, doi:10.1111/j.1365-2486.2008.01807.x, 2009.
Xie, Y., Xiong, Z., Xing, G., Yan, X., Shi, S., Sun, G., and Zhu, Z.: Source of nitrogen in wet deposition to a rice agroecosystem at Tai lake region, Atmos. Environ., 42, 5182–5192, doi:10.1016/j.atmosenv.2008.03.008, 2008.
Zhang, K., Wang, Y., Wen, T., Meslmani, Y., and Murray, F.: Properties of nitrate, sulfate and ammonium in typical polluted atmospheric aerosols (PM_{10}) in Beijing, Atmos. Res., 84, 67–77, doi:10.1016/j.atmosres.2006.05.004, 2007.
Zhang, Y., Liu, X. J., Fangmeier, A., Goulding, K. T. W., and Zhang, F. S.: Nitrogen inputs and isotopes in precipitation in the North China Plain, Atmos. Environ., 42, 1436–1448, doi:10.1016/j.atmosenv.2007.11.002, 2008.
Zhang, Y., Liu, J., Mu, Y., Pei, S., and Lun, X.: Emissions of nitrous oxide, nitrogen oxides and ammonia from a maize field in the North China Plain, Atmos. Environ., 45, 2956–2961, doi:10.1016/j.atmosenv.2010.10.052, 2011.
Zhao, X., Yan, X., Xiong, Z., Xie, Y., Xing, G., Shi, S., and Zhu, Z.: Spatial and temporal variation of inorganic nitrogen wet deposition to the Yangtze River Delta Region, China, Water Air Soil Poll., 203, 277–289, doi:10.1007/s11270-009-0011-2, 2009.
Zhao, Y., Duan, L., Xing, J., Larssen, T., Nielsen, C. P., and Hao, J.: Soil acidification in China: is controlling SO_2 emissions enough?, Environ. Sci. Technol., 43, 8021–8026, doi:10.1021/es901430n, 2009.
Zheng, X. H., Fu, C. B., Xu, X. K., Yan, X. D., Huang, Y., Han, S. H., Hu, F., and Chen, G. X.: The Asian nitrogen cycle case study, Ambio, 31, 79–87, doi:10.1579/0044-7447-31.2.79, 2002.

ACPD
12, 753–785, 2012

Table 1. Contribution of different pathways and species to the estimated total N deposition ($kg\,N\,ha^{-1}\,yr^{-1}$) in Northern China.

Location	Site	Total N deposition	Wet	Dry		Reduced N	Oxidized N
				Particle	Gas		
Urban	BJ	59.2 (5.7)b	47.2 %	9.5 %	43.4 %	72.1 %	27.9 %
	TJ	52.2 (5.6)b	34.8 %	9.9 %	55.4 %	78.4 %	21.6 %
Industrial	BD	58.3 (2.8)b	39.6 %	11.5 %	48.9 %	79.0 %	21.0 %
	TG	100.4 (14.4)a	28.1 %	5.4 %	66.5 %	86.7 %	13.3 %
	TS	59.9 (3.7)b	36.0 %	11.1 %	52.9 %	77.9 %	22.1 %
Suburban	YF	42.4 (7.0)c	48.8 %	11.9 %	39.3 %	70.6 %	29.4 %
	CZ	58.8 (6.0)b	38.4 %	11.0 %	50.7 %	82.1 %	17.9 %
Agricultural	LC	75.5 (6.1)a	29.4 %	9.4 %	61.3 %	87.5 %	12.5 %
	YC	70.7 (12.0)b	35.1 %	9.2 %	55.7 %	86.7 %	13.3 %
Rural	XL	28.5 (3.5)c	57.0 %	14.8 %	28.2 %	72.2 %	27.8 %
10-site-average		60.6 (19.6)	39.4 %	10.4 %	50.2 %	79.3 %	20.7 %

Standard deviation is in parentheses. Different letters in the "Total N deposition" column indicate significant difference between sites at $p < 0.05$. Definition of site codes is found in the footnotes of Fig. 1.

ACPD
12, 753–785, 2012

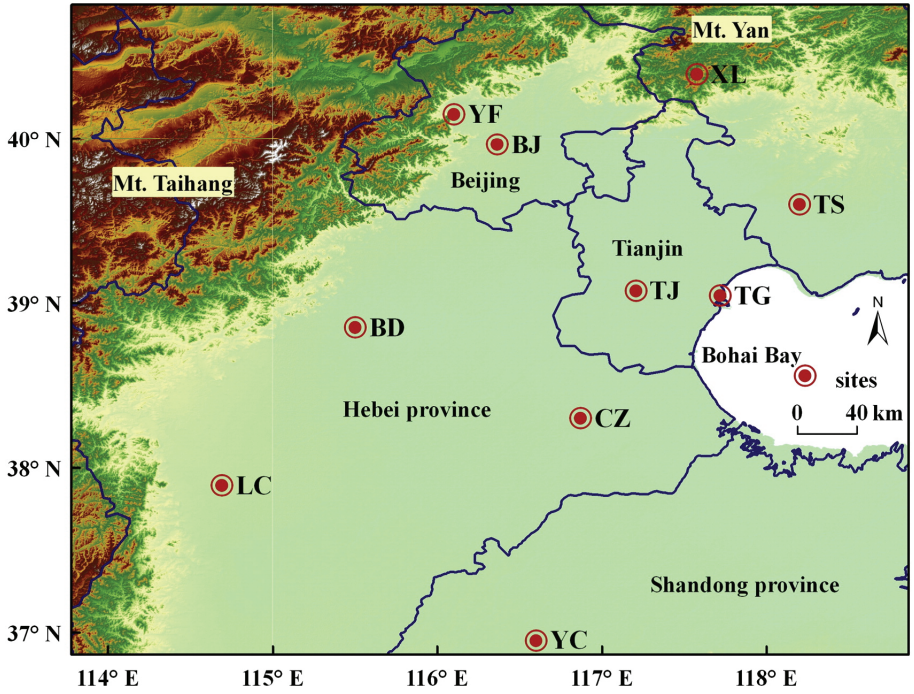

Fig. 1. Locations of the sampling sites in Northern China. Of the ten selected sites, two mega city sites are located in the Beijing (BJ, 39.96° N, 116.36° E) and Tianjin (TJ, 39.08° N, 117.21° E) downtown, two suburban sites at 2 km southeast away to the Cangzhou city (CZ, 38.30° N, 116.87° E) and at Yangfang (YF, 40.15° N, 116.10° E) which is 40 km northwest to the Beijing city, three industrial city sites in the center of Baoding city (BD, 38.85° N, 115.50° E), the coastal Tanggu (TG, 39.04° N, 117.72° E) area which is 30 km east to the Tianjin city and south to the Tangshan city (TS, 39.60° N, 118.20° E), two agricultural sites at Luancheng (LC, 37.89° N, 114.69° E) which is 4 km southeast to the Shijiazhuang city and 6 km southwest off the Yucheng city (YC, 36.85° N, 116.55° E), and one rural site at Xinglong (XL, 40.38° N, 117.57° E) on Mt. Yan with an elevation of 960 m a.s.l.

ACPD
12, 753–785, 2012

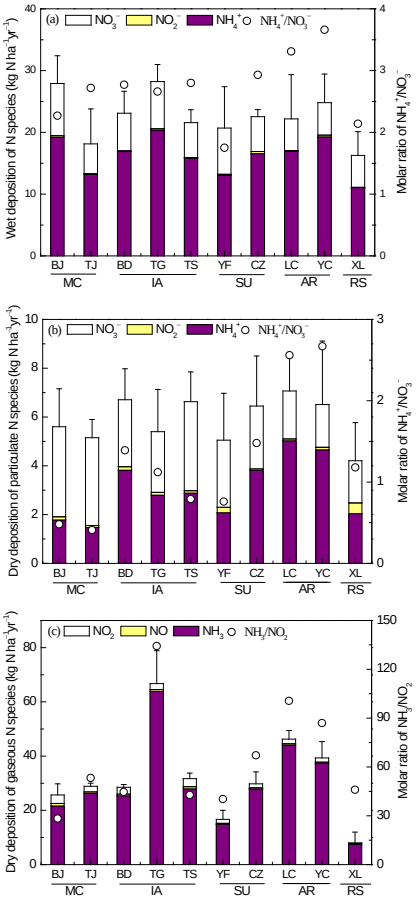

Fig. 2. Atmospheric deposition flux of nitrogen species at the ten selected sites in Northern China. The data shown are means of three-year observations, with the error bars denoting standard deviation. MC, IA, SU, AR and RS denote urban, industrial, suburban, agricultural and rural sites, respectively. Definition of site codes is found in the footnotes of Fig. 1.

ACPD
12, 753–785, 2012

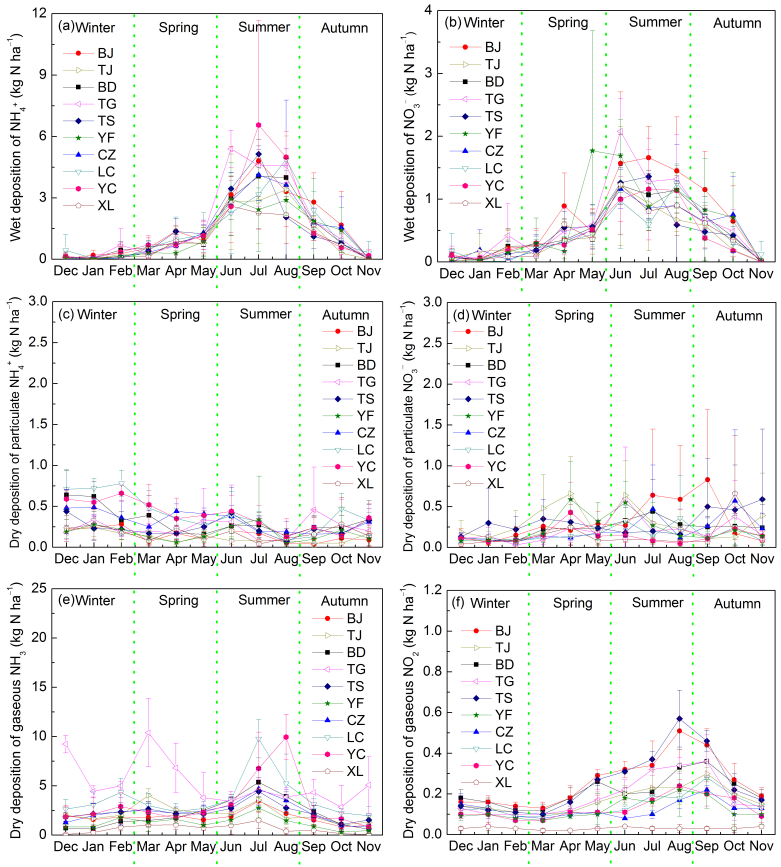

Fig. 3. Seasonal variations of the atmospheric deposition of nitrogen species at the ten selected sites in Northern China. The data shown are the monthly mean ± standard deviation of three-year observations (from December 2007 to November 2010). Definition of site codes is found in the footnotes of Fig. 1.

ACPD
12, 753–785, 2012

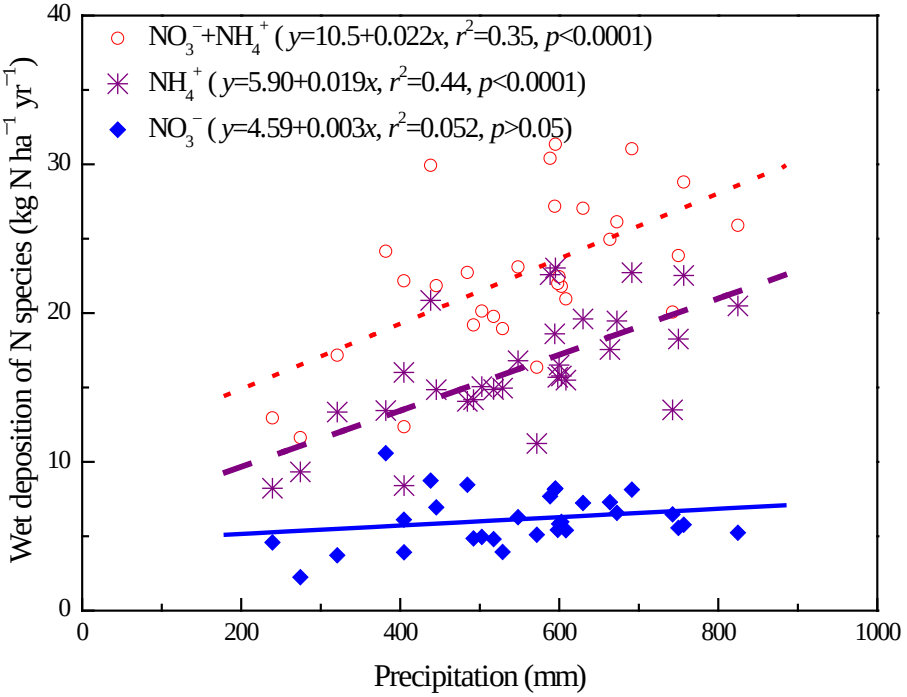

Fig. 4. Variation of the annual wet nitrogen deposition against precipitation in Northern China.

ACPD
12, 753–785, 2012

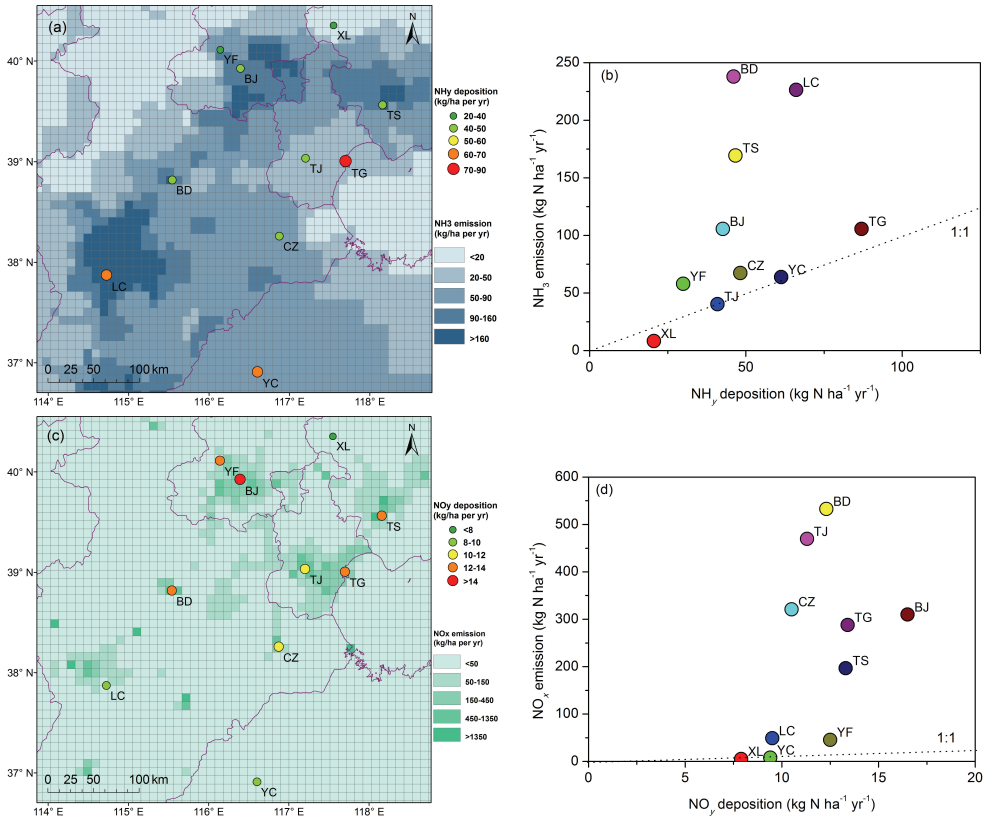

Fig. 5. Spatial variations of the atmospheric nitrogen deposition with emissions distributions in Northern China. The deposition data of NO_y (oxidized nitrogen) and NH_y (reduced nitrogen) are the annual mean of three-year observations (from December 2007 to November 2010). The emission data of NO_x and NH_3 are from 2008 with a resolution of $9 \times 9\,km^2$. Definition of site codes is found in the footnotes of Fig. 1.

ACPD
12, 753–785, 2012